

Coverage and Rate in MIMO Cellular Networks with Location-Aware Transmission Rank Selection

Afaq A. Lone, Abhishek K. Gupta, Harpreet S. Dhillon, Somya Sharma

Abstract—In this letter, we study the performance of a multiple-input multiple-output (MIMO) cellular network with location-aware transmission rank selection, where the number of transmit streams for every base-station (BS) and user equipment (UE) link is determined based on the average received power at the UE (hence, the *link distance*). We assume open-loop zero-forcing beam-forming (OL-ZFBF) at the receiver. We first develop a stochastic geometry based analytical framework for this setup by including the adaptive rank as a *mark* of each BS. Using this framework, we derive the coverage probability and spectral efficiency (SE) as a function of the rank selection threshold. Our analysis demonstrates that selecting transmission rank for each link on the basis of distance improves SE. We also investigate the tradeoff between coverage probability and SE.

Index Terms—Cellular networks, MIMO, stochastic geometry, Poisson point process, open loop zero-forcing beamforming.

I. INTRODUCTION

Network densification and multi-antenna transmission are two key ingredients of modern cellular networks. Given the variety of services and devices supported by these networks, there are many situations in which we cannot afford additional signaling overhead required to obtain channel state information (CSI) at the transmitter and hence have to limit ourselves to open-loop transmission techniques. A simple technique to harness multi-antenna transmission gains in the absence of CSI at the transmitter (CSIT) is to dynamically select the transmission rank for each BS-UE link based on the distance of the UE from the BS. While the link-level performance of this scheme is well-studied, the same is not true for its comprehensive system-level modeling and performance analysis, which is the main theme of this letter.

Prior Art. Over the past decade, stochastic geometry has emerged as a powerful tool for the system-level analysis of cellular networks. It has been particularly useful in accurately modeling irregular deployments resulting from network densification in heterogeneous cellular networks, e.g., see [1], [2]. These tools have also been extended to study various aspects of MIMO heterogeneous networks, e.g., see [3]–[5], where [3] derived upper bounds on coverage probability for different multi-antenna techniques and [4] investigated the impact of load balancing on the coverage and rate of these networks. The most relevant prior art for us in this direction is [5], which investigated the coverage probability in a MIMO heterogeneous cellular network with (open loop) multi-stream transmission to a single user using OL-ZFBF. However, all these works assume that the number of streams transmitted by each BS of a given tier is the same, which is overly simplistic from the perspective of modern cellular networks,

A. Lone, A. Gupta and S. Sharma are with IIT Kanpur, India. Email: {afaq, gkrabbi, somyas}@iitk.ac.in. H. S. Dhillon is with Wireless@VT, Department of ECE, Virginia Tech, USA. Email: hdhillon@vt.edu. The work of H. S. Dhillon was supported by the US NSF through grant CNS-2107276.

where BSs can decide the number of streams to be transmitted to the user (termed transmission rank) based on the channel conditions between BS and the user. In fact, this *transmission rank selection* feature also appears in the 3GPP LTE-Advanced and 5G standards. This rank selection can be facilitated by calculating a rank indicator (RI) based on the current channel at the UE and then feeding it back to the BS [6].

It is well-known that rank selection is useful in optimizing link performance by avoiding resource wastage resulting from transmitting too many streams on a weak MIMO channel on one hand and transmitting too little streams on a strong MIMO channel on the other [6], [7]. Even though this is easy to understand for a single link, it is not so in a network setting where transmission rank also impacts the interference statistics. While there are some simulation-based studies discussing the impact of rank selection [6], [8] on the network performance, this letter presents the first analytical system-level analysis of this setup. Because of the consideration of adaptive rank selection, the resulting stochastic geometry setup is different from the ones encountered in the past works. For example, the signal-to-interference ratios (SIRs) of different streams are correlated and also dependent on the serving BS's location, which requires careful treatment.

Contributions. In this letter, we develop a stochastic geometry based analytical framework to study the effect of dynamic rank selection in a cellular network with OL-ZFBF. In OL-ZFBF, ZFBF is performed at the UE having full CSI and hence CSIT is not assumed at the BS. Each BS decides the number of streams for its associated UE based on the average received power at the UE (equivalently based on the link distance). Key technical contributions of our analysis are the development of a tractable analytical approach which includes the effect of location-aware dynamic rank selection and the complete characterization of coverage probability and SE in terms of key system parameters (particularly the *selection distance threshold* used to determine the transmission rank). We also compute the optimal values of this threshold that maximize coverage and SE. Further, we discuss the trade off between coverage probability and SE, and investigate the optimal operating point to achieve the best trade-off.

Notation: $X \sim \Gamma(K)$ denotes that X is a Gamma random variable with shape K and rate 1. $B(a, b, z)$ is complementary incomplete Beta function *i.e.* $B(a, b, z) = \int_z^1 t^{a-1} (1-t)^{b-1} dt$. $W(\cdot)$ is the Lambert W function. $\mathcal{L}_X(s)$ denotes the Laplace transform (LT) of X .

II. SYSTEM MODEL

We consider the downlink of a MIMO cellular network, where the locations of the BSs are modeled as a PPP $\Phi = \{x_i\}$ with density λ . Here, x_i denotes the location of the i -th BS. The UEs are distributed as an independent and stationary point

process (PP) Φ_u with density λ_u . Each user connects to its closest BS. We assume a saturated traffic model where each BS has at least one UE to serve at all times. This can be justified by assuming $\lambda_u \gg \lambda$, which implies that the probability of finding an empty cell is very small. We further assume standard power-law path-loss model $\ell(r) = r^{-\alpha}$ with path-loss exponent $\alpha > 2$. We assume that each BS and UE is equipped with $M = 2$ antennas. Therefore, each UE forms a 2×2 MIMO system with its serving BS and hence the maximum number of streams supported for each user is 2. We further consider dynamic selection of the transmission rank such that the BS located at \mathbf{x}_i selects transmission rank n_i based on the average received power at the associated user. If the received power is above a threshold p_{th} , $n_i = 2$, otherwise $n_i = 1$. Due to the monotonicity of the path-loss function, $\ell(r)$, it translates to the following rule: $n_i = 2$ if $d_i < R$ and $n_i = 1$ if $d_i \geq R$ where d_i is the distance between the BS \mathbf{x}_i and its UE and $R = p_{\text{th}}^{-1/\alpha}$ is a design parameter (termed the *selection distance threshold*). Here, n_i can be seen as a *mark* for Φ , with $n_i \in \{1, 2\}$. The analysis can be extended to a general M with $1 \leq n_i \leq M$ [5] and more sophisticated RI based rank selection methods [6] at the expense of more complicated expressions and the possibility of obfuscating insights. Since the two-antenna setup is already rich enough to reveal the problem structure and key performance trends, the expressions for general M are not included due to space constraints.

We consider OL-ZFBF, where ZFBF is performed at the UE assuming perfect CSI, whereas CSIT is not required [9]. Along the same lines as [9], we assume that the BSs simply turn on one transmit antenna per stream and the transmit power is equally divided among streams, which are both justified in OL-ZFBF due to the unavailability of CSIT. As discussed in [9], turning on only the required number of antennas may also reduce the overall interference in the network. Further, we assume an independent Rayleigh fading channel between every transmitter-receiver antenna pair. Our analysis will focus on the typical user located to the origin, which connects to its closest BS located at \mathbf{x}_0 . The PDF of its distance $r_0 = \|\mathbf{x}_0\|$ from the user, is given as [2] $f_{r_0}(r) = 2\pi\lambda r e^{-\pi\lambda r^2} \mathbb{1}(r > 0)$. Let this BS be transmitting $n_0 \in \{1, 2\}$ streams. Based on the marks assigned to the BSs, we split the set of interfering BSs (*i.e.* $\Phi \setminus \{\mathbf{x}_0\}$) into two PPs, Φ_1 and Φ_2 , corresponding to $n_i = 1$ and 2, respectively. Hence, $\Phi = \Phi_1 \cup \Phi_2 \cup \{\mathbf{x}_0\}$. The received signal vector $\mathbf{z}_0 \in \mathbb{C}^{n_0 \times 1}$ is

$$\mathbf{z}_0 = \|\mathbf{x}_0\|^{-\frac{\alpha}{2}} \mathbf{h}_0 \mathbf{s}_0 + \sum_{\mathbf{x}_i \in \Phi_1} \|\mathbf{x}_i\|^{-\frac{\alpha}{2}} \mathbf{h}_i \mathbf{s}_i + \sum_{\mathbf{x}_i \in \Phi_2} \|\mathbf{x}_i\|^{-\frac{\alpha}{2}} \mathbf{h}_i \mathbf{s}_i.$$

Here, $\mathbf{h}_0 \in \mathbb{C}^{M \times n_0}$ is the fading channel matrix between serving BS \mathbf{x}_0 and the typical UE, $\mathbf{h}_i \in \mathbb{C}^{M \times n_i}$ is the fading channel matrix between the interfering BS at \mathbf{x}_i and the typical UE. Further \mathbf{s}_i of size $n_i \times 1$ is the signal vector transmitted by the i -th BS \mathbf{x}_i . When $n_i = 1$, only the first antenna is active, hence \mathbf{s}_i can be replaced with its first element s_i . We ignore thermal noise in this analysis. In OL-ZFBF, the received vector is multiplied with the zero-forcing beam-former, given as $(\mathbf{h}_0^H \mathbf{h}_0)^{-1} \mathbf{h}_0^H$ which cancels the inter stream interference completely at the cost of reduced degrees of freedom. Using

[9, Section II-A, Eq. (7)], the SIR for l -th stream is given as

$$\text{SIR}_l = \frac{\frac{1}{n_0} \|\mathbf{x}_0\|^{-\alpha} F_{0,l}}{I_{1,l} + \frac{1}{2} I_{2,l}} \quad (1)$$

$$\text{with } I_{1,l} = \sum_{\mathbf{x}_i \in \Phi_1} \|\mathbf{x}_i\|^{-\alpha} H_{i,l}, \quad I_{2,l} = \sum_{\mathbf{x}_j \in \Phi_2} \|\mathbf{x}_j\|^{-\alpha} H_{j,l}. \quad (2)$$

Here, $I_{m,l}$ denotes the sum interference from Φ_m for unit transmit power on the l -th stream, $F_{0,l} \sim \Gamma(m - n_0 + 1)$ is the fading power gain for the serving link and $H_{i,l} \sim \Gamma(n_i)$ is the fading power gain for the i -th interfering BS in Φ_m . We have $F_{0,l} \sim \Gamma(2)$ and $F_{0,l} \sim \Gamma(1)$ for the serving BS with one and two streams, respectively. Also, $H_{i,l}$'s are distributed as $\Gamma(1)$ and $\Gamma(2)$ for Φ_1 and Φ_2 , respectively [9, Eq.(9)]. For $n_0 = 2$, random variables F and H are independent across streams. However, SIR_1 and SIR_2 are not independent due to the presence of the same random variables $\{\mathbf{x}_i\}$ in path-loss terms $\|\mathbf{x}_i\|^{-\alpha}$.

III. PERFORMANCE ANALYSIS

In this section, we derive the coverage probability and spectral efficiency (SE) of the typical user.

A. Rank Distribution

We will first derive the distribution of n_i , *i.e.*, the probability that the typical BS is transmitting 1 or 2 streams. The approximate distribution of the distance between the typical BS and a user distributed uniformly at random in its association cell is given as $\mathbb{P}[u \geq r] = \exp(-1.28\pi\lambda r^2)$ [10]. Hence, the probability that the typical BS transmits only one stream is

$$p_1(\rho) = \mathbb{P}[u > R] = \exp(-1.28\pi\lambda R^2) = \exp(-1.28\rho), \quad (3)$$

where $\rho = \pi\lambda R^2$ is the normalized selection distance threshold and represents the average number of BSs in a circle of radius R . The underlying BS Poisson Voronoi tessellation induces dependence in the marks n_i and hence the PPs Φ_1 and Φ_2 . Handling this dependence exactly is intractable because of which we will assume that the marks are independent. This approximation does not affect the accuracy of the analysis as shown later in Fig. 1(a). Therefore, we can treat Φ_1 and Φ_2 as two independent PPPs with densities $\lambda_1(\rho) = p_1(\rho)\lambda$ and $\lambda_2(\rho) = p_2(\rho)\lambda$, respectively with $p_2(\rho) = 1 - p_1(\rho)$.

B. Coverage probability

We define the coverage probability as the probability that the SIR for all the streams is greater than the threshold τ *i.e.*

$$p_c(\tau) = \mathbb{E} \left[\prod_{l=1}^{n_0} \mathbb{1}(\text{SIR}_l \geq \tau) \right]. \quad (4)$$

This captures the fact that it will be meaningful to select two stream transmission only when both streams are successful. As n_0 depends on r_0 , (4) can be written as

$$p_c(\tau) = p_{c,1} + p_{c,2}$$

$$\text{with } p_{c,1} = \mathbb{E} [\mathbb{1}(\text{SIR}_1 \geq \tau) \mathbb{1}(r_0 > R)], \quad (5)$$

$$p_{c,2} = \mathbb{E} \left[\prod_{l=1}^2 \mathbb{1}(\text{SIR}_l \geq \tau) \mathbb{1}(r_0 \leq R) \right]. \quad (6)$$

These two terms are derived in the following Lemmas.

Lemma 1. *The coverage probability for the typical UE when it receives a single stream transmission is*

$$p_{c,1} = \int_R^\infty \mathbb{P}[SIR_1 \geq \tau | r_0] f_{r_0}(r) dr_0 \quad (7)$$

$$\text{with } \mathbb{P}[SIR_1 \geq \tau | r_0] = \mathcal{L}_I(r_0^\alpha \tau) - \frac{d}{dt} \mathcal{L}_I(tr_0^\alpha \tau) |_{t=1} \quad (8)$$

where $I = I_{1,1} + I_{2,1}/2$ is the sum interference for the active streams. See Appendix A for the proof.

Lemma 2. *The coverage probability for the typical user when it receives two stream transmission is*

$$p_{c,2} = \int_0^R \mathbb{P}[\cap_l (SIR_l \geq \tau) | r_0] f_{r_0}(r) dr_0 \quad (9)$$

$$\text{with } \mathbb{P}[\cap_l (SIR_l \geq \tau) | r_0] = \mathcal{L}_{I_1}(2\tau r_0^\alpha) \mathcal{L}_{I_2}(\tau r_0^\alpha) \quad (10)$$

where $I_m = I_{m,1} + I_{m,2}$ is the sum interference from Φ_m summed over both streams. See Appendix B for the proof.

To solve further, we require LT of various interference terms. Next, we provide a general result for the LT.

Lemma 3. *Given the serving BS is at a distance r_0 , the Laplace transform of interference I from BSs $\Phi' \sim \text{PPP}(\lambda)$ with effective fading $H \sim \Gamma(N)$ and unit transmit power, evaluated at $s = \tau r_0^\alpha$, is given as (proof in Appendix C)*

$$\mathcal{L}_I(\tau r_0^\alpha) = \mathbb{E}[e^{-\tau r_0^\alpha I}] = \exp(-\pi \lambda_m r_0^2 f_N(\tau)) \quad (11)$$

$$\text{where, } f_N(\tau) = \sum_{k=1}^N \binom{m}{k} q(N-k, k, \tau)$$

$$\text{with } q(x, y, z) = 2/\alpha(z)^{2/\alpha} B(x + 2/\alpha, y - 2/\alpha, 1/(1+z)).$$

Equipped with these results, we now provide the coverage probability expression in the following Theorem.

Theorem 1. *The coverage probability for the typical user is*

$$p_c(\tau, \rho) = p_{c,1} + p_{c,2}, \text{ with} \quad (12)$$

$$p_{c,1} = \int_\rho^\infty e^{-vA(\tau, \rho)} (1 + vB(\tau, \rho)) dv = \frac{e^{-\rho A}}{A^2} [A + B + AB\rho]$$

$$p_{c,2} = \int_0^\rho e^{-vC(\tau, \rho)} dv = (1 - e^{-\rho C(\tau, \rho)})/C(\tau, \rho),$$

where A, B and C are given as:

$$A(\tau, \rho) = p_1(\rho) f_1(\tau) + p_2(\rho) f_2(\tau/2) + 1, \quad (13)$$

$$B(\tau, \rho) = p_1(\rho) q(1, 1, \tau) + 2p_2(\rho) q(2, 1, \tau/2), \quad (14)$$

$$C(\tau, \rho) = p_1(\rho) f_2(2\tau) + p_2(\rho) f_4(\tau). + 1 \quad (15)$$

Proof: See Appendix D. ■

This analysis can also be extended to the case of $M > 2$. Here, the system will allow M possible ranks to transmit data. Therefore, we will have a $(M-1) \times 1$ threshold vector ρ for rank selection and Φ can be partitioned into M PPPs $\{\Phi_k\}$. The SINR coverage can be written as a summation of M terms, one corresponding to each of the possible ranks. Note that $F_{0,l} \sim \Gamma(M-L+1)$ and $H_{i,l} \sim \Gamma(n_i)$. Using steps similar to Appendix A, we can write each term in terms of LT of interference and its derivatives. Please see [11] for details. Terms A, B and C can be approximated as (see Appendix E):

$$A(\tau, \rho) \approx f_2(\tau/2) + 1 = f_1(\tau) + 1 = \tilde{A}(\tau), \quad (16)$$

$$B(\tau, \rho) \approx 2q(2, 1, \tau/2) = q(1, 1, \tau) = \tilde{B}(\tau), \quad (17)$$

$$C(\tau, \rho) \approx f_4(\tau) + 1 = f_2(2\tau) + 1 = \tilde{C}(\tau). \quad (18)$$

where $\tilde{A}, \tilde{B}, \tilde{C}$ are functions of only τ . Using this approximation, we can simplify (12) to get the following result (See Appendix F for the proof).

Corollary 1. *The coverage probability p_c is a decreasing function of ρ , therefore SIR coverage is highest when $\rho = 0$ which means that all users are allotted a single stream. Further, the maximum and minimum values of p_c are*

$$p_{c,\max}(\tau) \approx (\tilde{A}(\tau) + \tilde{B}(\tau))/\tilde{A}^2(\tau), \quad p_{c,\min}(\tau) \approx 1/\tilde{C}(\tau).$$

The optimality of single stream transmission from the SIR standpoint is not surprising. However, simultaneous transmission of two streams has the potential of providing higher data rate compared to a single stream transmission at the expense of a lower SIR. This is discussed next by analyzing SE.

C. Spectral Efficiency

The SE η is defined as the average number of bits successfully transmitted per unit time and unit bandwidth [12] i.e.

$$\eta(\tau, \rho) = \mathbb{E}[n_0 \log_2(1 + \tau) \mathbb{1}(\text{SIR} \geq \tau)] \quad (19)$$

Theorem 2. *The SE in the considered network is*

$$\eta(\tau, \rho) = \log(1 + \tau) p_{c,1}(\tau, \rho) + 2 \log(1 + \tau) p_{c,2}(\tau, \rho). \quad (20)$$

The optimal value of ρ that maximizes SE is calculated next.

Theorem 3. *The value of distance selection threshold ρ that maximizes the SE is*

$$\rho_{\text{opt}} \approx \frac{1}{\tilde{C} - \tilde{A}} \mathbb{W}\left(\frac{2\tilde{C} - \tilde{A}}{\tilde{B}} \exp\left(\frac{\tilde{C} - \tilde{A}}{\tilde{B}}\right)\right) - \frac{1}{\tilde{B}} \leq \frac{1}{\tilde{C} - \tilde{A} + \tilde{B}}. \quad (21)$$

Proof: The ρ_{opt} can be obtained by differentiating (20) with respect to ρ and equating it to zero, which gives

$$2e^{-\rho \tilde{C}} - e^{-\rho \tilde{A}}(1 + \rho \tilde{B}) = 0.$$

Solving the above equation we get the result in (21). The upper bound can be proven using concavity of \mathbb{W} . ■

Remark 1. *From Theorem 3, we can make the following observations: (i) The upper bound in (21) decreases with τ which indicates that the optimal value of ρ decreases with τ . (ii) Cor. 1 and Theorem 3 show that the values of ρ that maximize η and p_c are different. (iii) The optimal value of ρ does not depend on the BS density λ . Therefore, as the BS density increases, the distance threshold R decreases.*

The use of optimal ρ results in the following degradation and improvement in p_c and η

$$\Delta p_c = p_c(\tau, 0) - p_c(\tau, \rho_{\text{opt}})$$

$$= (1 - \kappa^{\tilde{A}})\tilde{B}/\tilde{A}^2 + (1 - 2\kappa^{\tilde{C}})/\tilde{A} - (1 - \kappa^{\tilde{C}})/\tilde{C}.$$

$$\Delta \eta = \eta(\tau, \rho_{\text{opt}}) - \eta(\tau, 0) = \left[(1 - \kappa^{\tilde{C}})/\tilde{C} - \Delta p_c\right] \log_2(1 + \tau).$$

$$\text{with } \kappa = \left[\tilde{B} \mathbb{W}(2(\tilde{C} - \tilde{A})/\tilde{B} e^{(\tilde{C} - \tilde{A})/\tilde{B}})/(2(\tilde{C} - \tilde{A}))\right]^{1/(\tilde{C} - \tilde{A})}.$$

We also give the expression of ergodic rate defined as $r_e = \mathbb{E}[n_0 \log_2(1 + \text{SIR})]$ in the following Theorem.

Theorem 4. The ergodic rate of the typical user is given as

$$r_e = \int_0^\infty p_{c,1}(2^t - 1) + 2p'_{c,2}(2^t - 1)dt,$$

where $p_{c,1}$ is given in Theorem 1 and $p'_{c,2}(\tau) = \frac{1-e^{-\rho A(2\tau,\rho)}}{A(2\tau,\rho)}$.

Proof: To compute ER, we first apply the total probability law over events $r_0 \leq R$ and $r_0 > R$. We then use the fact that $\mathbb{E}[X] = \int_0^\infty \mathbb{P}[X > x] dx$. The rest of the steps are similar to the proof of p_c . \blacksquare

IV. NUMERICAL RESULTS

Unless stated otherwise, we consider $\alpha = 3$, $\lambda = 10/km^2$ and $\lambda_u = 100/km^2$ for all our numerical results.

Fig. 1(a) presents the coverage probability p_c for different values of threshold radius R (equivalently p_1 or ρ). The close agreement between the theoretical and simulation results verifies the accuracy of independent marking assumption. Further, Fig. 1(a) shows that p_c is the highest when R is equal to 0 (i.e., each BS transmits a single stream) and lowest when each BS transmits two streams. This is consistent with the observations of [3]–[5] that the increasing multiplexing gain reduces coverage probability. Further, the coverage probability for the intermediate values of ρ remains between the two extremes $\rho = 0$ and $\rho \rightarrow \infty$, which is consistent with Cor. 1.

Fig. 1(b) shows the variation of SE with ρ . This shows the existence of optimal ρ that maximizes SE. The optimal ρ depends on τ and decreases with an increase in τ . This is consistent with Remark 1. Further, ρ_{opt} is remarkably close to the exact ρ that maximizes SE. This validates the easy-to-use approximations given in (16)–(18) and Theorem 3.

Fig. 2(a)–(b) present trade-off between p_c and η for $\rho = 0$ (which maximises p_c) and for $\rho = \rho_{opt}$ (which maximises η). Any $\rho > \rho_{opt}$ will decrease both p_c as well as η , and is hence not desirable. Further, we observe that as we increase ρ from 0 to ρ_{opt} the decrease in p_c is smaller than the increase in η especially for the higher values of τ . Therefore, it is desirable to operate near ρ_{opt} for moderate to high values of τ .

V. CONCLUSIONS

In this letter, we have analytically characterized the performance of a MIMO cellular network with location aware rank selection in terms of coverage, SE and ER. Several useful insights were obtained from these analytical expressions. For instance, we obtained an analytical characterization of ρ_{opt} , that maximizes SE. While this optimal value is naturally different from the one that maximizes coverage, we have argued that it is desirable to operate near ρ_{opt} for moderate to high values of SIR threshold, τ , to have the best tradeoff between coverage and SE. This work can be extended in multiple ways. First, one can extend this analysis to the case of general M , which is tedious but conceptually straightforward given the analysis presented here. An analytical investigation of multiuser MIMO with dynamic rank selection for each multiplexed user is an interesting future direction. A similar analysis can also be performed for a closed-loop systems with CSI available at both ends of the link, including the massive MIMO settings. However, the resulting analysis is expected to be significantly different due to technical difficulties in deriving the underlying channel distributions.

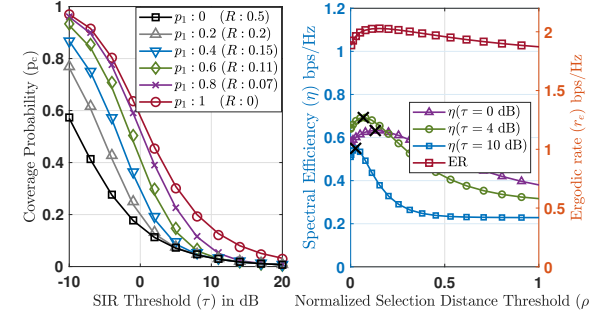


Fig. 1: Left: (a) Coverage probability for different values of threshold distance R . Solid lines represent analysis and markers represent simulation. Right: (b) Variation of SE with ρ for different values of τ . ρ_{opt} computed in (21) is shown by a \times on each plot.

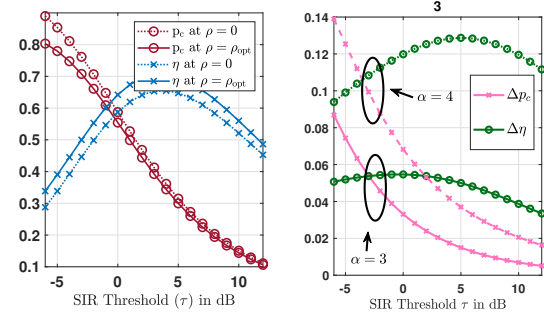


Fig. 2: Left: (a) Trade-off between p_c and η with τ for $\rho = 0$ and $\rho = \rho_{opt}(\tau)$. Right: (b) Variation of Δp_c and $\Delta \eta$ with τ .

APPENDIX A

From (5), $p_{c,1} = \int_0^\infty \mathbb{P}[\text{SIR}_1 \geq \tau | r_0] \mathbb{1}(r_0 > R) f_{r_0}(r) dr_0$

$$\text{where } \mathbb{P}[\text{SIR}_1 \geq \tau | r_0] = \mathbb{P}[r_0^{-\alpha} F_{0,1} / (I_1 + I_2/2) \geq \tau] = \mathbb{P}[F_{0,1} \geq \tau r_0^\alpha I_{1,1} + \tau r_0^\alpha I_{2,1}/2] = \mathbb{P}[F_{0,1} \geq \tau r_0^\alpha I]. \quad (22)$$

Since, $F_{0,1} \sim \Gamma(2)$, for a random variable y ,

$$\mathbb{P}[F_{0,1} \geq y] = \mathbb{E}_y [e^{-y}(1+y)] = \mathbb{E}_y [e^{-y}] - \frac{d}{dt} \mathbb{E}_y [e^{-yt}] |_{t=1}.$$

In (22), $y = \tau r_0^\alpha I$, therefore, $\mathbb{E}_y [e^{-yt}] = \mathcal{L}_I(\tau r_0^\alpha \tau)$. Substituting it back in (22) completes the proof.

APPENDIX B

From (6), $p_{c,2} = \int_0^R \mathbb{P}[\text{SIR}_1 \geq \tau, \text{SIR}_2 \geq |r_0|] f_{r_0}(r_0) dr_0$.

Since, for a given realization of Φ , SIR_1 and SIR_2 are independent, hence

$$\mathbb{P}[\cap_l (\text{SIR}_l \geq \tau) | r_0] = \mathbb{E}_\Phi \left[\prod_l \mathbb{P}[\text{SIR}_l \geq \tau | r_0, \Phi] \right]. \quad (23)$$

$$\begin{aligned} \text{Now, } \mathbb{P}[\text{SIR}_l \geq \tau | r_0, \Phi] &= \mathbb{P}[r_0^{-\alpha} F_{0,l}/2 / (I_{1,l} + I_{2,l}/2) \geq \tau] \\ &= \mathbb{P}[F_{0,l} \geq \tau r_0^\alpha (2I_{1,l} + I_{2,l})] = \mathbb{E} [e^{-2\tau r_0^\alpha I_{1,l} - \tau r_0^\alpha I_{2,l}} | r_0, \Phi] \end{aligned}$$

where the last step follows from $F_{0,l} \sim \Gamma(1)$. Now from (23),

$$\begin{aligned} \mathbb{P}[\cap_l \text{SIR}_i \geq \tau | r_0] &= \mathbb{E}_\Phi \left[\prod_l \mathbb{E} [e^{-\tau r_0^\alpha (2I_{1,l} + I_{2,l})} | r_0, \Phi] \right] \\ &= \mathbb{E}_\Phi [\mathbb{E} [\exp(-\tau r_0^\alpha (2I_1 + I_2)) | r_0, \Phi]]. \end{aligned} \quad (24)$$

Now, since each I_m is a function of Φ_m only, hence, from independence of Φ_m 's,

$$\mathbb{P}[\cap_l \text{SIR}_i \geq \tau | r_0] = \prod_m \mathbb{E}_{\Phi_m} [\exp(-\tau r_0^\alpha (2I_1 + I_2)) | r_0].$$

Now, using the definition of LT, we get the desired result.

APPENDIX C

From (2), the LT $\mathcal{L}_I(s)$ of I_m at $s = \tau r_0^\alpha$ is given as

$$\begin{aligned} \mathcal{L}_{I_m|r_0}(\tau r_0^\alpha) &= \mathbb{E} \left[e^{-\tau r_0^\alpha \sum_{z_i \in \Phi_m} \|z_i\|^{-\alpha} H_i \mathbb{1}(\|z_i\| > r_0)} \right] \\ &\stackrel{(a)}{=} \exp \left(-2\pi\lambda_m \int_{r_0}^\infty \left[1 - \mathbb{E}_H \left[e^{-\tau r_0^\alpha z^{-\alpha} H} \right] \right] zdz \right) \\ &\stackrel{(b)}{=} \exp \left(-2\pi\lambda_m \int_{r_0}^\infty \left[1 - (1 + \tau r_0^\alpha z^{-\alpha})^{-m} \right] zdz \right) \\ &\stackrel{(c)}{=} \exp \left(-\pi\lambda_m r_0^2 \tau^{\frac{2}{\alpha}} \int_{\tau^{-\frac{2}{\alpha}}}^\infty \left[1 - (1 + tv^{-\frac{\alpha}{2}})^{-m} \right] dv \right) \quad (25) \end{aligned}$$

where (a) from PGFL of PPP, (b) follows from moment generating function (MGF) of $H \sim \Gamma(m)$ and (c) follows by substituting $\tau^{\frac{2}{\alpha}} (r_0/z)^2 \rightarrow 1/v$. Now let

$$\begin{aligned} f_m(\tau) &= \tau^{2/\alpha} \int_{\tau^{-2/\alpha}}^\infty \left[1 - (1 + v^{-\alpha/2})^{-m} \right] dv \\ &\stackrel{(a)}{=} \tau^{\frac{2}{\alpha}} \sum_{k=1}^m \binom{m}{k} \int_{\tau^{-2/\alpha}}^\infty (v^{-\alpha/2})^k (1 + v^{-\alpha/2})^{-m} dv \\ &\stackrel{(b)}{=} \frac{2}{\alpha} \tau^{\frac{2}{\alpha}} \sum_{k=1}^m \binom{m}{k} \int_{\frac{1}{1+\tau}}^1 u^{m-k+\frac{2}{\alpha}-1} (1-u)^{k-\frac{2}{\alpha}-1} du \\ &= \sum_{k=1}^m \binom{m}{k} q(m-k, k, \tau) \end{aligned}$$

where, (a) follows from using binomial series, (b) follows from substituting $(1 + v^{-\alpha/2}) \rightarrow 1/u$. Now using $f_m(\tau)$ in (25) and putting $t = 1$, we get the desired result.

APPENDIX D

To derive p_c , we need to first derive the LT of I and I_m as defined in Lemma 1 and 2.

LT of I in Lemma 1 and $p_{c,1}$: Since $I = I_{1,1} + I_{2,1}/2$,

$$\begin{aligned} \mathcal{L}_I(r_0^\alpha \tau) &= \mathcal{L}_{I_{1,1}}(r_0^\alpha \tau) \mathcal{L}_{I_{2,1}}(r_0^\alpha \tau/2) \\ &\stackrel{(a)}{=} \exp(-\pi r_0^2 (\lambda_1 f_1(\tau) + \lambda_2 f_2(\tau/2))) \quad (26) \end{aligned}$$

where (a) follows from lemma 3. Further,

$$\frac{d}{dt} \mathcal{L}_I(tr_0^\alpha \tau) = \frac{d}{dt} \mathcal{L}_{I_{1,1}}(tr_0^\alpha \tau) \mathcal{L}_{I_{2,1}}(tr_0^\alpha \tau/2),$$

By differentiating (25) using Leibniz integral rule of differentiation under the integral sign, we get following result,

$$\begin{aligned} \frac{d}{dt} \mathcal{L}_I(tr_0^\alpha \tau) |_{t=1} &= \exp(-\pi r_0^2 (\lambda_1 f_1(\tau) + \lambda_2 f_2(\tau/2))) \\ &\times (\pi r_0^2 \{ \lambda_1 q(1, 1, \tau) + 2\lambda_2 q(2, 1, \tau/2) \}). \quad (27) \end{aligned}$$

Using results in (26) and (27), we get,

$$\begin{aligned} \mathbb{P}[\text{SIR} \geq \tau | r_0] &= \exp(-\pi r_0^2 (\lambda_1 f_1(\tau) + \lambda_2 f_2(\tau/2))) \\ &\times (1 + \pi r_0^2 \{ \lambda_1 q(1, 1, \tau) + 2\lambda_2 q(2, 1, \tau/2) \}). \end{aligned}$$

Using this result in (7), we get

$$\begin{aligned} p_{c,1} &= 2\pi\lambda \int_R^\infty \exp(-\pi\lambda r_0^2 (p_1 f_1(\tau) + p_2 f_2(\tau/2) + 1)) \\ &\times (1 + \pi\lambda r_0^2 \{ p_1 q(1, 1, \tau) + p_2 q(2, 1, \tau/2) \}) r_0 dr_0. \end{aligned}$$

Substituting $\pi\lambda r_0^2 \rightarrow v$, we get the desired result.

LT of I_m in Lemma 2 and $p_{c,2}$: Note that

$$I_m = \sum_l I_{m,l} = \sum_{z_i \in \Phi_m} \|z_i\|^{-\alpha} H_i$$

where, $H_i = H_{i,1} + H_{i,2} \sim \Gamma(2N_m)$ is the effecting fading. Therefore, from Lemma 3,

$$\mathcal{L}_{I_m}(\tau r_0) = \mathbb{E} [e^{-\tau r_0 I_m}] = \exp(-\pi\lambda_1 r_0^2 f_{2N_m}(\tau)).$$

Now, from (10), and noting $N_m = m$,

$$\mathbb{P}[\cap_i \text{SIR}_i \geq \tau | r_0] = \exp(-\pi r_0^2 \lambda_1 f_2(2\tau)) \exp(-\pi r_0^2 \lambda_2 f_4(\tau)).$$

Using this result in (9), we get

$$p_{c,2} = 2\pi\lambda \int_0^R \exp(-\pi\lambda r_0^2 (p_1 f_2(2\tau) + p_2 f_4(\tau) + 1)) r_0 dr_0$$

Substituting $\pi\lambda r_0^2 \rightarrow v$, we get the desired result.

APPENDIX E

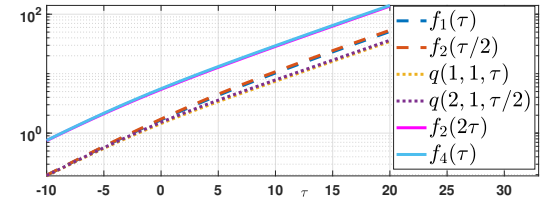


Fig. 3: Variations of f and q functions with respect to τ .

From Fig. 3, it can be seen that $f_1(\tau) \approx f_2(\tau/2)$, $q(1, 1, \tau) \approx 2q(2, 1, \tau/2)$ and $f_2(2\tau) \approx f_4(\tau)$. Applying these to (13)-(15) and noting $p_1 + p_2 = 1$, we get the desired result.

APPENDIX F

The local maxima/minima for p_c occurs at $\rho = \rho_0$ if

$$\frac{d}{d\rho} p_c(\tau, \rho)|_{\rho=\rho_0} = 0 \implies \exp((\tilde{C} - \tilde{A})\rho_0) = \tilde{B}\rho_0 + 1$$

Since $\tilde{C} > \tilde{A}$ (See Fig. 3), we get

$$\rho_0 = \frac{1}{\tilde{C} - \tilde{A}} \mathbb{W} \left(\frac{\tilde{C} - \tilde{A}}{\tilde{B}} \exp \left(\frac{\tilde{C} - \tilde{A}}{\tilde{B}} \right) \right) - \frac{1}{\tilde{B}} = \frac{1}{\tilde{C} - \tilde{A}} \left(\frac{\tilde{C} - \tilde{A}}{\tilde{B}} \right) - \frac{1}{\tilde{B}} = 0.$$

Further, since the $\frac{d p_c}{d \rho}$ is negative, p_c decreases with ρ .

REFERENCES

- [1] H. S. Dhillon, R. K. Ganti, F. Baccelli, and J. G. Andrews, "Modeling and analysis of K-tier downlink heterogeneous cellular networks," *IEEE J. Sel. Areas Commun.*, vol. 30, no. 3, pp. 550–560, April 2012.
- [2] J. G. Andrews, A. K. Gupta, A. Alammouri, and H. S. Dhillon, *An Introduction to Cellular Network Analysis using Stochastic Geometry*. Morgan Claypool, 2022.
- [3] H. S. Dhillon, M. Kountouris, and J. G. Andrews, "Downlink MIMO HetNets: Modeling, ordering results and performance analysis," *IEEE Trans. Wireless Commun.*, vol. 12, no. 10, pp. 5208–22, Oct. 2013.
- [4] A. K. Gupta, H. S. Dhillon, S. Vishwanath, and J. G. Andrews, "Downlink multi-antenna heterogeneous cellular network with load balancing," *IEEE Trans. Commun.*, vol. 62, no. 11, pp. 4052–4067, Nov. 2014.
- [5] M. G. Khoshkholgh, K. G. Shin, K. Navaie, and V. Leung, "Coverage performance in multistream MIMO-ZFBF heterogeneous networks," *IEEE Trans. Veh. Technol.*, vol. 66, no. 8, pp. 6801–18, Aug. 2017.
- [6] Z. Bai, C. Spiegel, G. H. Bruck, P. Jung, M. Horvat, J. Berkmann, C. Drewes, and B. Gunzelmann, "On the physical layer performance with rank indicator selection in LTE/LTE-Advanced system," in *Proc. IEEE PIMRC Workshops*, 2010, pp. 393–398.
- [7] Evolved Universal Terrestrial Radio Access, "Physical layer procedures (release 8)," *Technical Specification, 3GPP TS*, vol. 36, p. V8, 2009.
- [8] X. Chen, A. Benjebbour, Y. Lan, A. Li, and H. Jiang, "Impact of rank optimization on downlink non-orthogonal multiple access (NOMA) with SU-MIMO," in *Proc. IEEE ICCS*, 2014, pp. 233–237.
- [9] R. H. Y. Louie, M. R. McKay, and I. B. Collings, "Open-loop spatial multiplexing and diversity communications in ad hoc networks," *IEEE Trans. Info. Theory*, vol. 57, no. 1, pp. 317–344, Jan. 2011.
- [10] P. D. Mankar, P. Parida, H. S. Dhillon, and M. Haenggi, "Distance from the nucleus to a uniformly random point in the 0-cell and the typical cell of the Poisson–Voronoi tessellation," *J. Statistical Physics*, vol. 181, no. 5, pp. 1678–1698, Oct 2020.
- [11] A. Lone, "Coverage analysis in MIMO cellular networks with location aware transmission rank selection," Master's thesis, IITK, 2022. [Online]. Available: <http://home.iitk.ac.in/%7egkrabhi/thesis/afaq.pdf>
- [12] M. G. Khoshkholgh and V. Leung, "On the performance of MIMO-SVD multiplexing systems in HetNets: A stochastic geometry perspective," *IEEE Trans. Veh. Technol.*, vol. 66, no. 9, pp. 8163–8178, Sept. 2017.